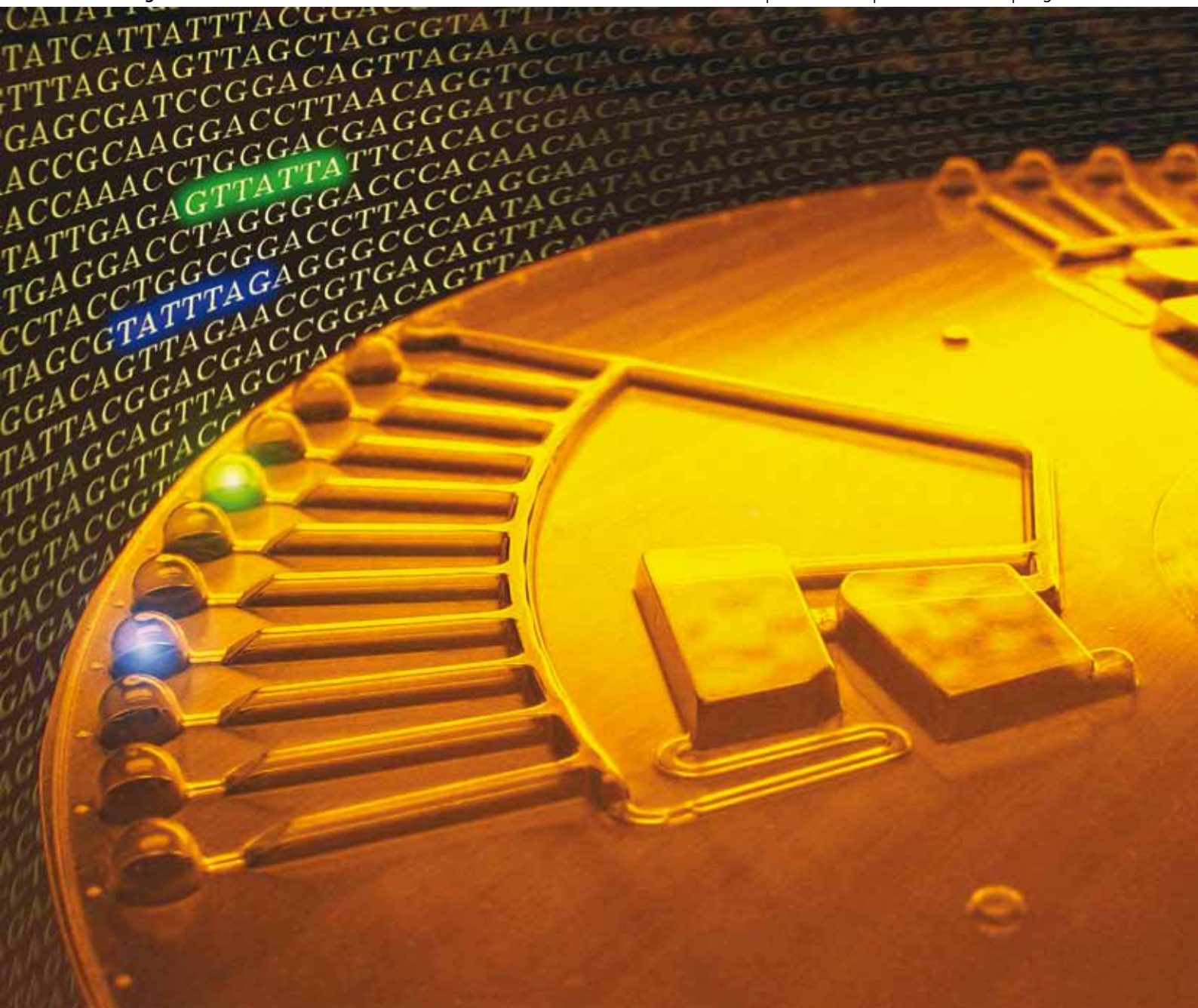


Lab on a Chip

Micro- & nano- fluidic research for chemistry, physics, biology, & bioengineering

www.rsc.org/loc

Volume 10 | Number 19 | 7 October 2010 | Pages 2481–2636



ISSN 1473-0197

RSC Publishing

Focke *et al.*
Microstructuring of polymer films

van Steijn *et al.*
Predictive model for bubbles

Celebrating
10
Years of publishing



1473-0197(2010)10:19;1-1

Microstructuring of polymer films for sensitive genotyping by real-time PCR on a centrifugal microfluidic platform

Maximilian Focke,^a Fabian Stumpf,^a Bernd Faltin,^a Patrick Reith,^a Dylan Bamarni,^a Simon Wadle,^a Claas Müller,^{bc} Holger Reinecke,^{bcd} Jacques Schrenzel,^{ef} Patrice Francois,^e Daniel Mark,^d Günter Roth,^{ad} Roland Zengerle^{*acd} and Felix von Stetten^{ad}

Received 8th April 2010, Accepted 15th June 2010

DOI: 10.1039/c004954a

We present a novel process flow enabling prototyping of microfluidic cartridges made out of polymer films. Its high performance is proven by implementation of a microfluidic genotyping assay testing 22 DNA samples including clinical isolates from patients infected by methicilin-resistant *Staphylococcus aureus* (MRSA). The microfluidic cartridges (disks) are fabricated by a novel process called microthermoforming by soft lithography (μ TSL). Positive moulds are applied allowing for higher moulding precision and very easy demoulding when compared to conventional microthermoforming. High replication accuracies with geometric disk-to-disk variations of less than 1% are typical. We describe and characterise fabrication and application of microfluidic cartridges with wall thicknesses <188 μ m thus enabling efficient thermocycling during real-time polymerase chain reaction (PCR). The microfluidic cartridges are designed for operation in a slightly modified commercial thermocycling instrument. This approach demonstrates new opportunities for both microfluidic developments and well-established laboratory instruments. The microfluidic protocol is controlled by centrifugal forces and divides the liquid sample parallelly into independent aliquots of 9.8 μ l (CV 3.4%, $N = 32$ wells). The genotyping assays are performed with pre-stored primers and probes for real-time PCR showing a limit of detection well below 10 copies of DNA per reaction well ($N = 24$ wells in 3 independent disks). The system was evaluated by 44 genotyping assays comprising 22 DNA samples plus duplicates in a total of 11 disks. The samples contained clinical samples of seven different genotypes of MRSA as well as positive and negative controls. The results are in excellent agreement with the reference in microtubes.

Introduction

The field of lab-on-a-chip^{1,2} is very application-oriented and aims at integration of new assays and thus enhanced utility for users in laboratories³ or at the point of care.⁴ The fabrication of microfluidic chips made of polymers is already well-established,⁵ especially by employing elastic materials like polydimethylsiloxane⁶ (PDMS) or thermoplastic materials.⁷ The latter are frequently processed by either hot embossing⁸ or injection moulding⁹ which allows high throughputs and thus cost-efficient mass production. Apart from that, processes like blow moulding and thermoforming¹⁰ of thermoplastic foils are massively employed in industrial sectors like food¹¹ and pharmaceutical¹² packaging. However, their impact on microfabrication and application of

lab-on-a-chip systems has been modest up to now although particularly the use of thermoplastic foils promises particularly attractive benefits for developers and users.¹³ For instance, microthermoforming uniquely enables fabrication of three-dimensional, almost uniformly thin-walled structures.¹⁴ Thin walls are particularly important for efficient thermal cycling as required in PCR.¹⁵ The time for heat transfer through a foil can be described by the diffusion equation and is inversely proportional to the square of the foil thickness.¹⁶ Additionally, the low mass of foil-based cartridges leads to a low moment of inertia. This is beneficial in centrifugal microfluidics where rotational acceleration and deceleration are used for liquid handling.^{17,18}

The principles of microthermoforming are well described, *e.g.* by Truckenmüller *et al.*^{19,20} So far, the capabilities of this process are limited because replication of delicate structures like sharp corners and defined edges was found to be unattainable.¹⁴ This is particularly true for so-called negative (female) moulds that can be used to pattern the later outside of microfluidic geometries. A suitable workaround is application of so-called positive (male) moulds. These are distinguished from negative moulds by their elevated structures that pattern the later inside of microfluidic channel geometries. We have recently pioneered in microthermoforming of polymer foils with such positive moulds.²¹ However, these moulding tools were fabricated by complex and time-consuming UV-LIGA and electroplating.²²

In order to overcome all these drawbacks and to provide sufficiently microstructured polymer foils for microfluidic applications,

^aLaboratory for MEMS Applications, Department of Microsystems Engineering (IMTEK), University of Freiburg, Georges-Koehler-Allee 106, 79110 Freiburg, Germany. E-mail: zengerle@imtek.de

^bLaboratory for Process Technology, Department of Microsystems Engineering (IMTEK), University of Freiburg, Georges-Koehler-Allee 106, 79110 Freiburg, Germany

^cCentre for Biological Signalling Studies (bioss), University of Freiburg, Germany

^dHSG-IMIT, Wilhelm-Schickard-Straße 10, D-78052 Villingen-Schwenningen, Germany

^eGenomic Research Laboratory, University of Geneva Hospitals, Rue Gabrielle-Perret-Genti 4, 1211 Geneva 14, Switzerland

^fClinical Microbiology Laboratory, University of Geneva Hospitals, Rue Gabrielle-Perret-Genti 4, 1211 Geneva 14, Switzerland

we developed the approach of microthermoforming by soft lithography (μ TSL) that applies elastic positive moulds known from conventional soft lithography.^{23,24} A master tool is cast with PDMS which is used as mould insert for microthermoforming. Due to the flexibility of both the cast PDMS mould and the foil, demoulding is possible even with orthogonal walls and without the need for draft angles or bevels.²⁵ This feature is crucial for facilitation and acceleration of construction and fabrication of master tools.

In this paper we explain how such cartridges (disks) can be fabricated by the μ TSL approach. Furthermore, we demonstrate genotyping by real-time PCR on a centrifugally actuated microfluidic disk. The assay is performed with pre-stored specific primers and probes as well as clinical, genomic DNA samples that were isolated and purified from swabs of patients infected with methicilin-resistant strains of *Staphylococcus aureus* (MRSA).

The microfluidic cartridges are particularly designed for integration in a slightly modified commercial thermocycling device (Rotor-Gene 2000 by Corbett Research Pty Ltd, now Qiagen GmbH). This standard lab instrument is thus “upgraded” by microfluidic process integration and automation. The approach of upgrading commercial laboratory equipment is intended to drastically facilitate development and commercialisation of lab-on-a-chip applications and is expected to largely increase market acceptance. In fact, researchers and developers usually engineer both a microfluidic chip and an appropriate processing or readout instrument.^{26,27} Also most manufactures of commercial lab-on-a-chip systems like Agilent (2100 Bioanalyzer) or 3M (Integrated Cycler) chose the same approach so far. Examples for the upgrading approach^{28,29} are hardly found although commercial devices like thermocyclers, fluorimeters or lab centrifuges could efficiently be enhanced by microfluidics.

Experimental setup

Disk design

Our foil cartridges (Fig. 1a) are circularly shaped disks and designed for centrifugal microfluidics. Each disk comprises four

identical and independent segments. Each segment (Fig. 1b) has an inlet chamber that is connected to a sloping feed channel with finger-like metering chambers. Distribution of the sample liquid can be improved by the slope of the channel. As a consequence, metering chambers become wider with decreasing length in order to keep the metering volume constant.

On the outer diameter, there are eight reaction wells and a reservoir for waste liquid. Each metering chamber is separated from the adjacent reaction well by a passive, centrifugo-pneumatic valve.³⁰ Air displacement by liquid flow is realised by a closed-loop ventilation. The full disk diameter is 130 mm.

The disks are designed for application in a Rotor-Gene 2000 thermocycling instrument. Its heating and cooling mechanism is based on convection of hot and cold air, respectively. Therefore, the disks require through holes to allow for sufficient air circulation (Fig. 1a). In its standard configuration, up to 72 PCR microtubes are inserted in a rotary holder that constantly rotates around an axis. Real-time detection of fluorescence signals takes place under rotation and is realised by excitation from underneath and a sideward detection unit. The modification of the instrument refers to an additional relay to increase the rotational speed discretely from standard 6.6 to 27.2 Hz. Further, the microtube holder is replaced by a custom-made, light-weight adaptor for fixation and alignment of microfluidic disks in the device (Fig. 2).

Fabrication process

In order to fabricate a microfluidic cartridge, a computer aided design (CAD) is generated (AutoCAD, Autodesk). The CAD drawing is transferred to a milling machine (Minimill, Minitech) to process a 4.0 mm thick polymethylmethacrylate (PMMA) plate.³¹ The milled PMMA master is cast with a special grade of PDMS (Elastosil RT-607, Wacker Chemie) and cured at 80 °C for 30 minutes (Fig. 3a). After demoulding, the PDMS mould has a thickness of 3.5 mm plus the elevated (positive) structures of the milled (negative) PMMA master. In order to obtain

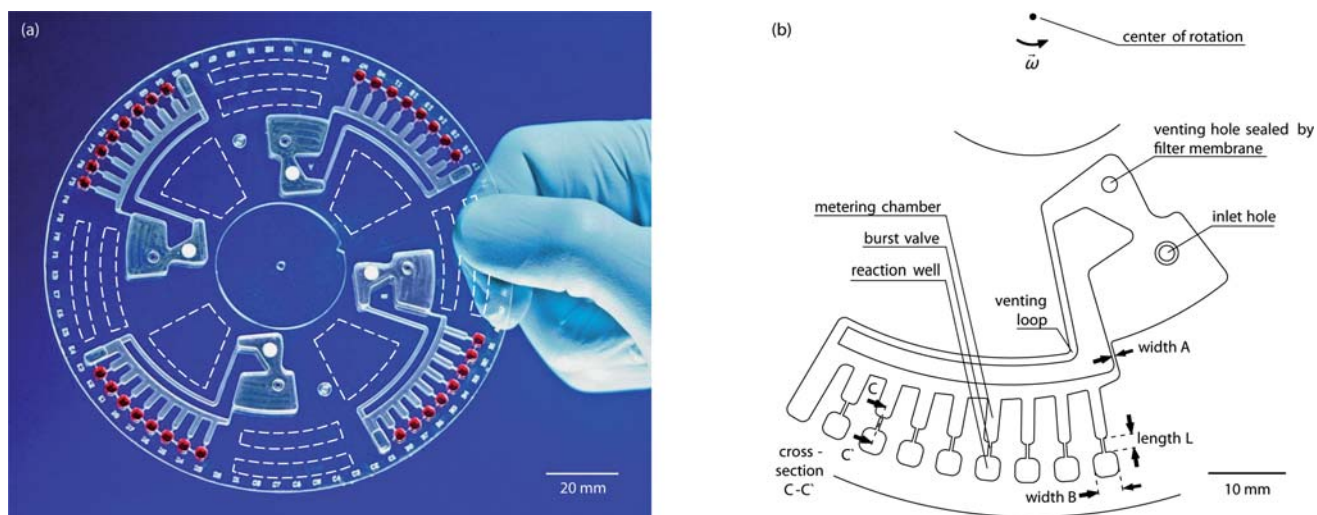


Fig. 1 Design of the foil cartridge. (a) Photograph of a foil disk (reaction wells are highlighted with a dye, contours of through holes for air flow are indicated as dashed lines); and (b) CAD drawing of a segment with microfluidic elements, sense of rotation ω and characteristic geometries (widths A and B, length L, and cross-section C-C').



Fig. 2 Assembly of the microfluidic foil cartridge in the modified centrifugal thermocycler Rotor-Gene 2000 (open top cover position).

a defined condition of the tool, it is post-cured at 200 °C and 1 kPa for one hour in order to avoid outgassing of remaining monomers in the PDMS matrix during later thermoforming processes.

Then, the PDMS mould is placed in a holder of a hot embossing machine (HEX01, Jenoptik Germany) which is equipped with an additional nitrogen feed-in. Tool and tool holder are covered by the substrate, a cyclic olefin polymer foil (COP, ZF14, Zeon Chemicals) with thickness 188 μm (Fig. 3b). The polymer foil features a glass transition temperature of 135 °C (FP90 DTA, Mettler Toledo) and transparency of approximately 93% transmission for visible light (UV 300, Unicam). It is applied due to its beneficial properties like thermal and mechanical stability, high transparency and biological inertness.^{32,33}

First, the tool holder is heated to a temperature of 130 °C. Then, the process chamber is evacuated to 0.1 kPa. The tool holder is heated further to 190 °C while the crossheads of the machine simultaneously start closing slowly until the foil is tightly clamped by the tool holder and upper crosshead (Fig. 3c). At the moulding temperature, nitrogen slowly pressurises the space over the foil to 210 kPa while the space under the foil remains at 0.1 kPa. The pressure difference presses the warm and soft foil onto the PDMS surface and replicates its topography to allow precise moulding (Fig. 3d). Hold time is 15 minutes. After cooling, venting and opening of the machine, the polymer foil can be demoulded from the PDMS mould (Fig. 3e).

Preparation of microfluidic cartridges

Microfluidic genotyping cartridges are equipped with dehydrated biological reagents for pre-storage. After sealing and cutting, filter membranes are attached.

For pre-storage of dry PCR reagents, a 0.8 μl mixture of gene-specific primers and TaqMan probe is spotted in each reaction well and dehydrated for 1 h at room temperature in the dark. Each reaction well comprises primers and probes for exactly one specific DNA target.

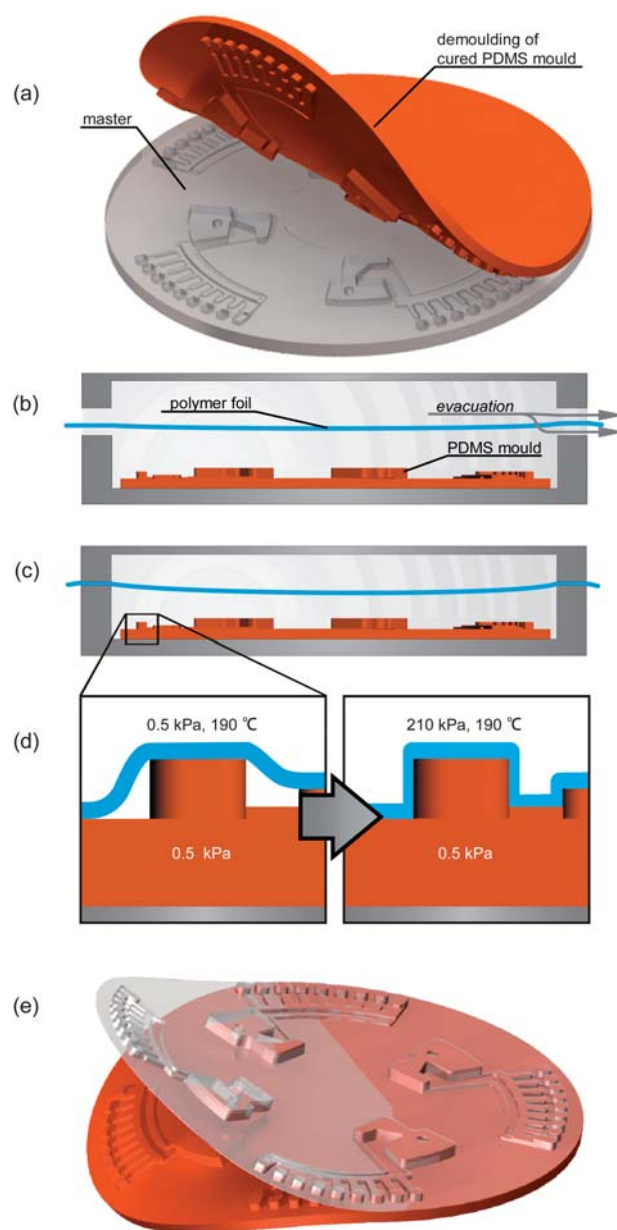


Fig. 3 Process flow for the formation of COP foils. (a) Fabrication of the PDMS mould; (b) assembly in a modified hot embossing machine and evacuation; (c) clamping of the foil in vacuum; (d) moulding of the foil through application of a pressure difference at moulding temperature; and (e) demoulding after cooling, venting and opening of the process chamber.

The disks are sealed with pressure sensitive adhesive foils (no. 900320, HJ Bioanalytik) which are typically used for sealing of microwell plates. The adhesive of the sealing film is silicone based and releases the adhesive only upon mechanical pressure (*i.e.* in direct contact with the foil substrate). Neither inhibition of the assay nor any case of leakage did occur with the applied sealing film. However, the cartridges are not hermetically sealed: according to the Clausius–Clapeyron equation, air expansion in the cartridge during later thermocycling leads to a drastic gas pressure increase up to 260 kPa (absolute) at 95 °C. This pressure increase would cause delamination of the sealing layer.

Therefore, we provide each segment with a 2.0 mm venting hole to ensure atmospheric pressure during thermocycling. In order to prevent DNA contaminations, each venting hole is sealed with a hydrophobic membrane (GORE™ Medical Membranes MMT-314, W. L. Gore & Associates, Inc.) that filters aerosols of 100 nm diameter with a 99.99% efficiency (material datasheet). No case of DNA contamination was observed in any of our experiments which will be discussed later in this paper.

Laser cutting (PLS 3.60, Universal Laser Systems) is applied to cut the disks in a circular shape and to provide alignment and inlet holes as well as through holes for sufficient air flow during thermocycling.

Sample loading

Insertion of a sample liquid is a main issue for all laboratory applications, especially in the context of prevention of cross-contaminations as well as sample integrity. However, operator interfaces are often disregarded in the design of microfluidic chips: Zhang and Xing³⁴ list only one out of 44 reviewed PCR chips with a sample loading feature although problems with DNA contamination and bubble generation have been reported relating to sample insertion. They also recommend sealing of inlet holes by a tape in order to decrease risk of DNA contamination. However, adhesive tapes can delaminate if a liquid film of a (usually) wetting PCR buffer remains on the sealing surface (Fig. 4a). Therefore, our inlets feature a novel design to avoid such effects. The inlets are located in a depression at a lower level than the sealing surface (Fig. 4b). The hole diameter is 2.0 mm, depth and width of the depression are 2.5 mm and 4.0 mm, respectively. Additionally, it is recommended to apply hydrophobic pipette tips (so-called low retention tips) in order to further reduce contamination risks during sample loading.

Centrifugal liquid handling

Centrifugal forces are used for microfluidic unit operations like transport, metering and separation. We have just recently reported on a new type of passive valve³⁰ which is applied here in combination with a distribution channel and metering chambers

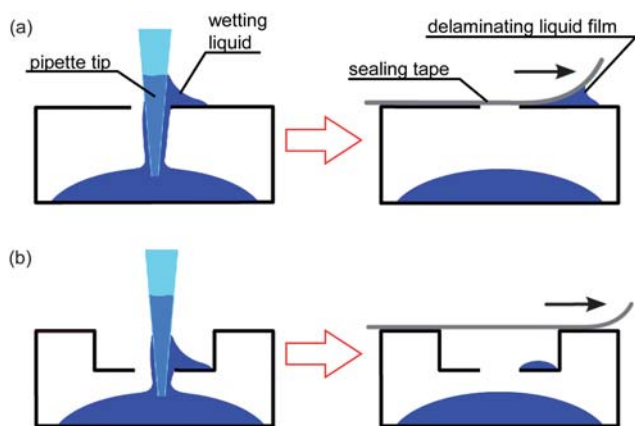


Fig. 4 Method for sealing inlets after insertion of highly wetting liquids (not to scale). (a) Sealing tape is wetted by remaining liquid and can thus delaminate. (b) The novel inlet design prevents wetting of sealing surfaces and allows robust sealing of inlet holes.

(Fig. 1b).³⁵ The valving principle is based on a counter pressure of compressed air in the receiving (but unvented) reaction well.

A liquid volume of 90 μl is inserted in each segment on the disk. After sealing of the inlet holes, the samples are aliquoted into eight adjacent metering chambers with a nominal volume of 10 μl at a rotational frequency of 6.6 Hz. An excess amount of 10 μl improves liquid handling and is collected in the adjacent waste reservoir located behind the metering chambers. The passive valves prevent filling of the reaction wells until unidirectional and alternating rotational frequencies between 6.6 and 27.2 Hz are applied (ramps of 6.6 Hz s^{-1}).³⁰ The alternation is repeated ten times. Once the reaction wells are filled, the system is in a stable equilibrium. Stopping or spinning at any frequency does not change the position of the aliquots. Furthermore, all aliquots are separated from each other so that no liquid film connects the samples. Aliquoting is controlled by a supplementary relay in the device.

PCR setup

The applied PCR mix is based on a commercially available buffer solution (1 \times , RealMasterMix with ROX, 5Prime, Germany). Further additives are target-specific primers (300 nM each), target-specific TaqMan probe (200 nM), bovine serum albumin (BSA, 0.3%, Carl Roth, Germany) and salmon sperm DNA (1 ng μl^{-1} , Sigma Aldrich, Germany). We apply 10 μl reactions and prepare sample volumes of 90 μl per microfluidic segment. In order to prove feasibility of the system, we primarily used the exfoliatin toxin A³⁶ (ExfA) gene that is present in some methicillin-resistant *S. aureus*³⁷ (MRSA) strains as target for PCR amplification (primers and probe sequences in respective literature). Genotyping of other MRSA subtypes will be discussed later.

Reference PCR is conducted in the same Rotor-Gene device with standard microtubes and the respective mix. The temperature protocol for PCR in foil cartridge (set points) comprises an activation step at 95 $^{\circ}\text{C}$ (110 s) and 50 subsequent thermocycles including a melting step at 95 $^{\circ}\text{C}$ (20 s) and annealing step at 57 $^{\circ}\text{C}$ (40 s) with subsequent fluorescence readout. For better comparability, the temperature protocol for reference PCR in microtubes is identical as the one used with the foil disk.

Results and discussion

Process characteristics

The main criteria for process characterisation were dimensional variations of the replicated foils and their deviation to the dimensions of the master. Further, wall thickness should not become too thin in order to conserve mechanical stability of the cartridge as well as preferably uniform heat transfer during later thermocycling.

The dimensions of characteristic geometries (widths A and B and length L, cf. Fig. 1b) are measured in 10 foil cartridges (Tesa Visio 300, Tesa Switzerland). Comparing the sizes of characteristic geometries between master and replicated foils (Table 1), the differences below 16 μm remain negligible as they do not affect the performance of this application.

The variations of the characteristic geometries in the 10 replicates are below 3 μm which is just slightly more than the

Table 1 Characteristic geometries in master tool and 10 replicates

Geometry ^a	Dimensions and measurement errors of PMMA master tool/ μm	Dimensions and variations of 10 foil replicates/ μm
Width A	386 (± 1)	382 (± 2)
Width B	3093 (± 1)	3078 (± 3)
Length L	1918 (± 1)	1930 (± 1)

^a cf. Fig. 1b.

resolution capacities of the measurement equipment (systematic variation $\pm 1 \mu\text{m}$).

A close-up of a passive valve channel is depicted in a SEM image (Fig. 5a). Sharp edges and even details like the replicated cutter paths are visible. Cutter grooves in the master with roughnesses in the range of approximately $\pm 1.3 \mu\text{m}$ (Zygo NewView 5022) are replicated in the foils in virtually equal quality.

Polymer foils are biaxially stretched during the thermoforming process. Usually, a high uniformity of foil thickness is desired in the field of thermoforming.¹⁰ However, it is inevitable to obtain thinning of the foil material. The lateral elongation in x and perpendicular y direction goes along with a reciprocal decrease of foil thickness when a constant density of the foil during the whole process is assumed (with mass and thus volume remaining unchanged).³⁸ A polymer foil was patterned by a laser printer with a fine grid (edge lengths 0.5 mm) in order to visualise the effects of stretching due to lateral elongation during the foil replication. Stretching along the vertical sidewalls of a reaction well is shown in Fig. 5b. In vertical direction the factor of stretching amounts to an approximate average of 1.3 based on the initial edge length of the printed grid (arrow in Fig. 5b). The corresponding wall thickness is depicted in a cross-sectional view of the perpendicular plane C–C' (Fig. 5c). The cavity bottom remains at approximately 80% of initial foil thickness while the sidewalls and rims are stretched down to $50 \mu\text{m}$ thickness in

corners. However, this does not affect mechanical stability for laboratory handling. A further beneficial feature of the process is its capability to mould straight and orthogonal walls without the need for draft angles or bevels since the flexible PDMS mould allows easy demoulding.

The described μTSL process chain takes less than one working day starting from a CAD scratch and including micromachining and casting of the master. Replication of foils takes approximately 30 minutes which is mainly due to warming and cooling phases of the machine. One PDMS mould can be used for far more than 140 replications.

Liquid handling

The crucial aspects in liquid handling are primarily sample insertion as well as reliable and precise aliquoting. Also the properties of the sample liquid influence liquid handling. In our case, the applied buffer solution showed a static contact angle of 66° on COP (OCA 15+, DataPhysics Instruments) which is relatively high compared to several other PCR buffers (contact angles as low as 25°). The inlet proved feasible in terms of resealing in 400 of 400 cases without a single failure. When this design element was omitted, resealing failed regularly even with application of hydrophobic (low retention) pipette tips. Therefore, the inlet design is essential if the hole has to be resealed by tape after filling.

It was feasible to aliquot liquid samples equally into eight reaction wells each. The passive valves feature suitable burst frequencies of 13 to 15 Hz depending on the hydropneumatic pressure induced by the filling height in the respective metering chambers. The resulting liquid volume in each reaction well was determined by observation of the relative filling level of each reaction well in relation to its actual volume which was measured beforehand (Tesa Visio 300).³⁰ The average volume of aliquots is $9.8 \mu\text{l} \pm 3.4\%$ non-systematic variation ($N = 32$ wells). The systematic deviation to the nominal volume of $10 \mu\text{l}$ is 2%. As a reference the standard EN ISO 8655 for multi-channel piston pipettes demands a systematic deviation of less

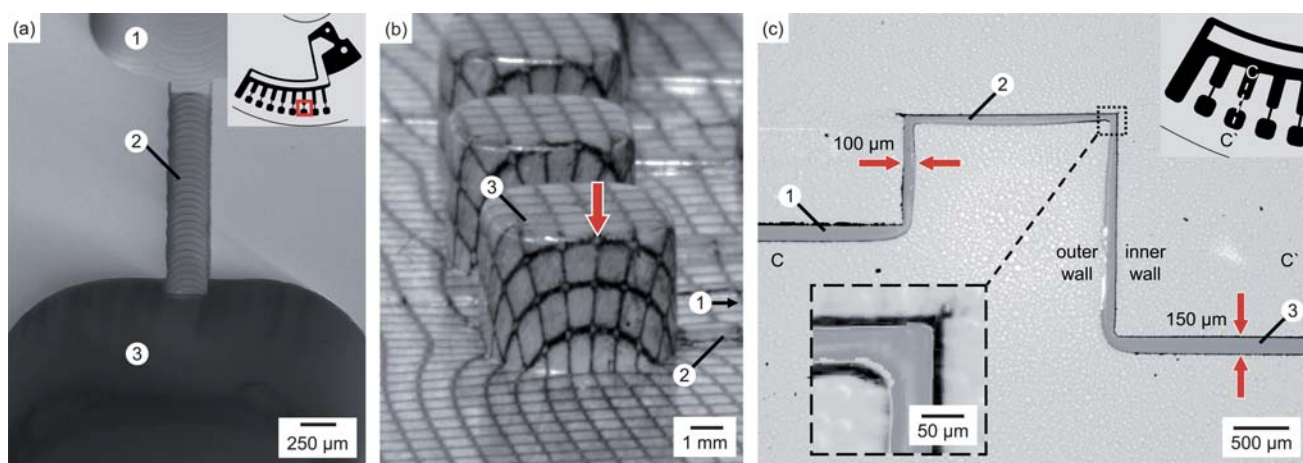


Fig. 5 Details of thermoforming results. The numbers depict microfluidic structures like metering chamber (1), passive valve (2) and reaction well (3). (a) SEM image of a microfluidic channel on a foil disk. (b) Visualisation of stretching by a printed grid (initial edge length 0.5 mm). The arrow points in a direction of uniaxial stretching by a factor of 1.3 over a reaction well with height 2.0 mm. (c) Micrograph image of a reaction well (cross-section C–C'). Sharp edges on the channel inside and orthogonal walls without draft angles are feasible.

than 2.4% and a non-systematic variation lower than 1.6% for nominal volumes of 10 μl . However, our achieved precision is fully acceptable for the requirements of the presented real-time genotyping assay. In case a significantly different PCR buffer is applied, a redesign of the centrifugo-pneumatic valve might be necessary. Burst frequencies particularly depend on the surface tension of the sample liquid and geometric properties like cross-section of the passive valve channel and the volume of the reaction wells.³⁰

Real-time PCR

The main characteristics of assays for nucleic acid analysis by real-time PCR are sensitivity (lower limit of detection of DNA copies), specificity (capability to detect one specific DNA sequence in a surplus of other DNA), reaction efficiency (probability of duplication of a specific DNA sequence within each PCR cycle), intra-disk variation (range of threshold cycles for replicates on disk) and generally disk-to-disk variation (reproducibility) of all these parameters.

In a first experiment, sensitivity was examined in a total of three foil disks (Fig. 6a). We selected exfoliatin toxin A (ExfA) as target sequence. Each of the three disks comprised 4 separate segments that were each filled with a sample of specific DNA concentration. Each disk contained one segment with a concentration of (statistically) 3.5 copies per reaction well and one segment with a no template control (NTC). Each of the remaining segments was filled with samples containing 35, 350, 3500 or 35 000 copies of target DNA per reaction well, respectively. ExfA-specific primers and probes were dehydrated in each reaction well. The results of the real-time detection are displayed as standard curves (Fig. 6a). Amplification and detection of less than 10 copies per reaction well are feasible in our system and were performed successfully in the respective segments in each of the three foil disks.

The same experiment was conducted in PCR microtubes as a reference. The variation of obtained threshold cycles (c_T) per concentration is compared between experiments on disk and

reference in tubes. The variation of threshold cycles in the disk is below 1.5 cycles for less than 10 DNA copies per reaction and below 0.5 cycles for more than 10 000 copies per reaction.

The efficiency of PCR amplification is determined by the slope m in the standard curve with change of threshold cycle c_T and change of \log (copy number)

$$m = \frac{\Delta c_T}{\Delta \log(\text{copy number})} \quad (1)$$

The reaction efficiency E is hence calculated as

$$E = (10^{-1/m}) - 1 \quad (2)$$

An efficiency of 100% is equivalent to a doubling of amplicons in every thermocycle. The amplification efficiencies on disk were 83% (Disk 1 with 3.5/35/350 DNA copies per reaction well), 90% (Disk 2 with 3.5/3500/35 000 DNA copies per reaction well), and 97% (Disk 3 with 3.5/35/3500 DNA copies per reaction well). The respective efficiency of reference PCR in microtubes was 74% (thermocycling conditions identical to disk protocol). The inferior efficiency of the reference PCR is attributed to suboptimal thermocycling conditions by heat convection. The regimes of air flow are very different for the foil disks and the standard rotor, respectively.

Cross-contamination of reactions by carryover of DNA is a permanent risk in PCR analysis. A highly sensitive PCR setup can be contaminated by a single DNA copy. Since our reaction wells are only spatially and not hermetically separated from each other, there is a theoretical risk of well to well contamination. Therefore, we examined the occurrence of carryover from well to well during thermocycling by dehydrating high DNA copy numbers (350 000 copies of subtype ExfA each) in wells 1, 3 and 5. Wells 2, 4 and 6 in between were left empty (see schematic in Fig. 6b). Wells 7 and 8 served as references with lower copy numbers of 350 and 35 copies, respectively. This scheme was parallelly repeated in all four segments of three disks. The wells were flushed with a PCR reaction mix containing only specific primers and probes but no target DNA. Then, real-time PCR

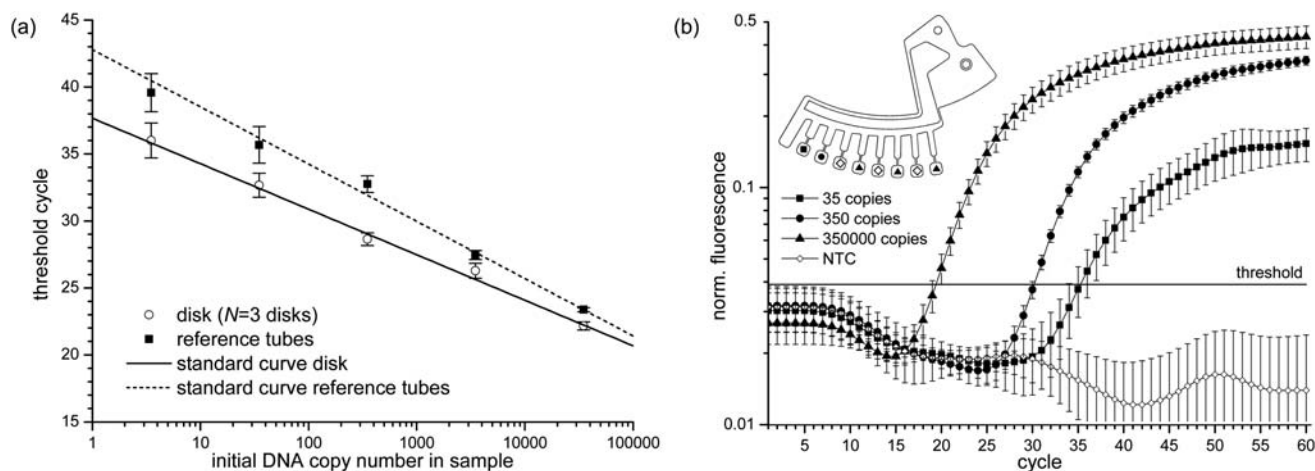


Fig. 6 Results of real-time PCR on a foil disk. (a) Threshold cycles and standard curves of 3 foil disks with varying copy numbers and a reference in standard tubes. Amplification of less than 10 copies per reaction is feasible. (b) Examination of cross-contamination across the reaction wells. High amounts of DNA do not contaminate adjacent wells with NTCs as NTC signals remain below threshold.

Table 2 Results of genotyping assay. The signs indicate true positive (+), true negative (–), false positive (p), and false negative (n) amplification

Sample	ExfA	ExfB	PVL	TSST-1	SCCmec I	SCCmec II	SCCmec IV	Lambda
1	+	–	–	–	–	–	–	–
2	+	+	–	–	–	–	–	–
3	–	–	n	–	–	–	–	–
4	–	–	–	+	–	+	–	–
5	–	–	–	–	+	–	–	–
6	–	–	–	+	–	+	–	–
7 ^a	–	–	–	–	–	–	–	–
8	–	+	–	–	–	–	–	–
9	–	–	n	–	–	–	+	–
10	–	–	–	–	+	–	–	–
11	–	–	–	–	–	+	–	–
12	–	–	–	+	–	+	–	–
13	+	+	–	–	–	–	–	–
14	–	–	n	–	+	–	–	–
15	–	–	–	–	+	–	–	–
16	–	–	n	–	–	+	–	–
17	–	–	–	–	–	+	+	–
18	–	–	–	–	+	+	–	–
19	+	–	–	–	–	–	–	–
20 ^b	–	–	–	–	–	–	–	+
21 ^c	–	–	n	–	–	–	–	–
22 ^d	–	–	–	–	–	–	–	–

^a Sample contained degraded DNA of SCCmec type IV and could thus not be amplified on disk and in reference tubes. ^b Feasibility of positive control: sample contained DNA of Lambda. ^c Negative control: sample contained DNA of SCCmec type V. ^d Negative control: sample contained DNA of *E. coli*.

was performed. The NTC samples did not generate any signal even after 60 thermocycles while the samples with 350 000, 350 and 35 copies were amplified as expected (Fig. 6b).

DNA carryover could not be detected despite the fact that a weight loss of approximately 5% of liquid was observed due to evaporation during thermocycling. In comparison, 24 standard microtubes initially filled with 10 μ l of PCR buffer each lost around 8% of weight based on the initial amount of liquid after 50 thermocycles. We conclude that there is practically no effect of DNA copies leaving the disk through the pressure balance air hole. In addition, the air hole is about 35 mm away from the nearest reaction well (nearly twice the distance between two wells). Potential aerosol transfer is further constricted by narrow-necked channels and the hydrophobic filter membrane.

Specificity is demonstrated in a genotyping assay with genomic DNA isolated from patients infected with different subtypes of MRSA. Seven respective genetic subtypes were examined (primer and probe sequences in respective literature): exfoliatin toxin A³⁶ (ExfA), exfoliatin toxin B³⁶ (ExfB), staphylococcal toxic shock syndrome toxin³⁶ (TSST-1), Pantón–Valentine leukocidin³⁹ (PVL), staphylococcal cassette chromosome *mec*³⁹ (SCCmec) type I, type II and type IV. DNA samples were provided and prepared by the University Hospitals of Geneva, Switzerland.

A total of 11 disks were prepared comprising 44 independent microfluidic structures. Respective primers and probes were pre-stored in each structure so that each genetic subtype could be detected in one reaction well. Additionally, primers and probes for MRSA-unrelated Lambda phage DNA were pre-stored in one reaction well per structure in order to provide possibility to include a positive reaction control. A total of 22 samples were examined in duplicates, *i.e.* a total of 44 genotyping assays. Results are summarized in Table 2.

The clinical samples comprised single- and multilocus genotypes of MRSA (*i.e.* a sample containing genetic sequences of

more than one specific subtype) as sometimes prevalent in clinical settings. One sample contained genomic DNA of *Escherichia coli* and another one contained DNA from SCCmec type V as negative controls. Both were tested true-negatively. One sample contained degraded DNA and could thus not be sufficiently tested. Further, it was found that the applied PCR mixture was not capable to amplify the PVL gene target (neither on disk nor properly in reference tubes). Hence, when compared to references, all 22 out of 22 samples were correctly examined by on-disk genotyping in 44 independent assays. These results show that high specificity is provided with our system.

The time for sample-in to result after 50 thermocycles is approximately 110 minutes for both the foil disk and the standard microtubes. This is owed to the holding times as well as the heating and cooling rates of the instrument. The duration for thermocycling is in good average compared to the state of the art of commercial thermocycling machines.^{40,41}

Foil disks are exposed to varying temperature conditions during thermocycling which can lead to slight distortions of the cartridges. The distortions are mainly based on the difference between the thermal expansion coefficients of the COP substrate foil and the self-adhesive sealing foil. However, this effect does not interfere the readout process as the customized cartridge holder in the thermocycling device sufficiently clamps the foil disks.

Conclusions and outlook

We have shown feasibility of advanced microthermoforming by soft lithography (μ TSL) and further demonstrated suitability of microfluidic foil cartridges for centrifugally actuated liquid handling and subsequent sensitive nucleic acid analyses.

The presented prototyping process combines advantages of soft lithography and positive tool design. It is not required to integrate draft angles or bevels in the tool because the flexible foil

can be easily demoulded from the soft PDMS moulds. Thus, construction and fabrication are facilitated and accelerated. The production process is very robust and yields a disk-to-disk variation below 3 µm in characteristic geometries like channel widths.

A commercially available thermocycling instrument was equipped with a custom-made disk adaptor and an additional relay to change rotational speeds of the spinning motor. These small modifications allowed upgrading of an existing laboratory instrument by integration of microfluidic automation. This concept allows drastical facilitation in development of lab-on-a-chip devices.

We have further demonstrated that the fabricated foil cartridges are suitable for microfluidic unit operations like transport, separation and metering as well as performance of a genotyping assay with real-time PCR. A novel operator interface allows insertion of highly wetting liquids. The design of the inlet holes prevents delamination of the sealing tape after liquid dispensing thus reducing risk of DNA contamination.

A genotyping assay was realised by implementation of real-time PCR on a centrifugal microfluidic platform. The platform enables parallel handling of four independent samples and detection of up to 8 different genes. The limit of detection is below 10 DNA copies per reaction well. Clinical samples containing DNA from various MRSA strains were analysed in our system with absolute accordance to the reference system thus implying suitability for clinical applications.

In the near future, we intend to enhance the presented system by integration of further microfluidic unit operations and more complex biochemical assays. In the long run, we envision upscaling of the microthermoforming process in order to make disks available for testing in a broader field of applications.

Acknowledgements

The research leading to these results has received funding from the European Community's Sixth Framework Programme (FP6) under contract no. 37957 (project MagRSA) and funding from the German Federal Ministry of Economics and Technology via grants of the German Federation of Industrial research Associations AIF under contract no. 15838N (project BlisterLab). The authors thank John Corbett (of the former Corbett Research Pty Ltd) for supporting this work by providing the Rotor-Gene 2000 instrument.

References

- 1 A. G. Crevillen, M. Hervas, M. A. Lopez, M. C. Gonzalez and A. Escarpa, *Talanta*, 2007, **74**(3), 342–357.
- 2 D. Mark, S. Haeberle, G. Roth, F. von Stetten and R. Zengerle, *Chem. Soc. Rev.*, 2010, **39**, 1153–1182.
- 3 T. A. Franke and A. Wixforth, *ChemPhysChem*, 2008, **9**(15), 2140–2156.
- 4 J. Kling, *Nat. Biotechnol.*, 2006, **24**(8), 891–893.
- 5 H. Becker and C. Gartner, *Anal. Bioanal. Chem.*, 2007, **390**(1), 89–111.
- 6 S. K. Sia and G. M. Whitesides, *Electrophoresis*, 2003, **24**(21), 3563–3576.
- 7 M. Hecke and W. K. Schomburg, *J. Micromech. Microeng.*, 2004, **14**(3), R1–R14.
- 8 J. M. Li, C. Liu, H. C. Qiao, L. Y. Zhu, G. Chen and X. D. Dai, *J. Micromech. Microeng.*, 2008, **18**(1), 015008.
- 9 U. M. Attia, S. Marson and J. R. Alcock, *Microfluid. Nanofluid.*, 2009, **7**(1), 1–28.
- 10 J. L. Throne, in *Technology of Thermoforming*, Hanser Publications, Cincinnati, 1996.
- 11 J. H. Han, in *Innovations in Food Packaging*, Elsevier Academic Press, London, 2005.
- 12 E. J. Bauer, in *Pharmaceutical Packaging Handbook*, 1st edn, Informa Healthcare USA, New York, 2009.
- 13 M. Focke, D. Kosse, C. Müller, H. Reinecke, R. Zengerle and F. von Stetten, *Lab Chip*, 2010, **10**(11), 1365–1386.
- 14 M. Worgull, in *Hot Embossing—Theory and Technology of Microreplication*, 1st edn, William Andrew, Burlington, 2009.
- 15 G. Y. Jia, J. Siegrist, C. W. Deng, J. V. Zoval, G. Stewart, R. Peytavi, A. Huletsky, M. G. Bergeron and M. J. Madou, *Colloids Surf., B*, 2007, **58**(1), 52–60.
- 16 Y. C. Lin, C. C. Yang and M. Y. Huang, *Sens. Actuators, B*, 2000, **71**(1–2), 127–133.
- 17 M. Grumann, A. Geipel, L. Riegger, R. Zengerle and J. Duerée, *Lab Chip*, 2005, **5**(5), 560–565.
- 18 S. Lutz, V. Reitenbach, D. Mark, J. Duerée, R. Zengerle and F. von Stetten, in *Proceedings of the 12th International Conference on Miniaturized Systems for Chemistry and Life Sciences*, ed. L. E. Locascio, M. Gaitan, B. M. Paegel and D. J. Ross, Chemical and Biological Microsystems Society, San Diego, 2008, pp. 748–750.
- 19 R. Truckenmüller, S. Giselbrecht, C. van Blitterswijk, N. Dambrowsky, E. Gottwald, T. Mappes, A. Rolletschek, V. Saible, C. Trautmann, K. F. Weibezahn and A. Welle, *Lab Chip*, 2008, **8**, 1570–1579.
- 20 R. Truckenmüller and S. Giselbrecht, *IEE Proc. Nanobiotechnol.*, 2004, **151**(4), 163–166.
- 21 A. Disch, H. Reinecke and C. Mueller, in *Proc. IEEE EMBS*, ed. A. Dittmar and J. Clark, IEEE, Lyon, 2007, pp. 6322–6325.
- 22 R. Jurischka, C. Blattert, I. Tahhan, C. Mueller, A. Schoth and W. Menz, in *Proc. SPIE Int. Soc. Opt. Eng.*, ed. I. Papautsky and I. Chartier, SPIE, San Jose, CA, USA, 2005, pp. 65–72.
- 23 Y. N. Xia and G. M. Whitesides, *Angew. Chem., Int. Ed. Engl.*, 1998, **37**(5), 551–575.
- 24 J. A. Rogers and R. G. Nuzzo, *Mater. Today*, 2005, **8**(2), 50–56.
- 25 P. Kumaresan and P. K. Wright, *Int. J. Comput. Integr. Manuf.*, 2005, **18**(1), 1–14.
- 26 A. F. Sauer-Budge, P. Mirer, A. Chatterjee, C. M. Klapperich, D. Chargin and A. Sharon, *Lab Chip*, 2009, **9**, 2803–2810.
- 27 J. Kim, D. Byun, M. G. Mauk and H. H. Bau, *Lab Chip*, 2009, **9**(4), 606–612.
- 28 A. P. Wong, M. Gupta, S. S. Shevkoplyas and G. M. Whitesides, *Lab Chip*, 2008, **8**(12), 2032–2037.
- 29 L. Riegger, M. Grumann, J. Steigert, S. Lutz, C. P. Steinert, C. Mueller, J. Viertel, O. Prucker, J. Ruhe, R. Zengerle and J. Duerée, *Biomed. Microdevices*, 2007, **9**(6), 795–799.
- 30 D. Mark, T. Metz, S. Haeberle, S. Lutz, J. Duerée, R. Zengerle and F. von Stetten, *Lab Chip*, 2009, **9**, 3599–3603.
- 31 F. Bundgaard, G. Perozziello and O. Geschke, *Proc. Inst. Mech. Eng., Part C*, 2006, **220**(11), 1625–1632.
- 32 J. Y. Shin, J. Y. Park, C. Y. Liu, J. S. He and S. C. Kim, *Pure Appl. Chem.*, 2005, **77**(5), 801–814.
- 33 W. D. Niles and P. J. Coassin, *Assay Drug Dev. Technol.*, 2008, **6**(4), 577–590.
- 34 C. S. Zhang and D. Xing, *Nucleic Acids Res.*, 2007, **35**(13), 4223–4237.
- 35 S. Lutz, P. Weber, M. Focke, B. Faltin, J. Hoffmann, C. Müller, D. Mark, G. Roth, P. Munday, N. Armes, O. Piepenburg, R. Zengerle and F. von Stetten, *Lab Chip*, 2010, **10**(10), 887–893.
- 36 P. Francois, S. Harbarth, A. Huyghe, G. Renzi, M. Bento, A. Gervais, D. Pittet and J. Schrenzel, *Emerging Infect. Dis.*, 2008, **14**(2), 304–307.
- 37 H. F. Chambers and F. R. Deleo, *Nat. Rev. Microbiol.*, 2009, **7**(9), 629–641.
- 38 L. R. Schmidt and J. F. Carley, *Polym. Eng. Sci.*, 1975, **15**(1), 51–62.
- 39 P. Francois, G. Renzi, D. Pittet, M. Bento, D. Lew, S. Harbarth, P. Vaudaux and J. Schrenzel, *J. Clin. Microbiol.*, 2004, **42**(7), 3309–3312.
- 40 E. van Pelt-Verkuil, A. van Belkum and J. P. Hays, in *Principles and Technical Aspects of PCR Amplification*, Springer Netherlands, 2008, vol. 332.
- 41 Y. H. Kim, I. Yang, Y. S. Bae and S. R. Park, *Biotechniques*, 2008, **44**(4), 495–505.